NASA TN D-279

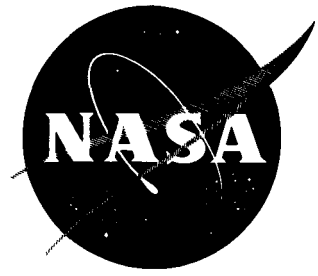

TECHNICAL NOTE

D-279

OPERATIONAL METHOD OF DETERMINING INITIAL CONTOUR OF AND PRESSURE FIELD ABOUT A SUPERSONIC JET

By Gerald W. Englert

Lewis Research Center
Cleveland, Ohio

NATIONAL AERONAUTICS AND SPACE ADMINISTRATION

WASHINGTON April 1960

NATIONAL AERONAUTICS AND SPACE ADMINISTRATION

TECHNICAL NOTE D-279

OPERATIONAL METHOD OF DETERMINING INITIAL CONTOUR OF AND PRESSURE FIELD ABOUT A SUPERSONIC JET

By Gerald W. Englert

SUMMARY

Simple expressions for estimating the initial contour of a jet exhausting into a supersonic stream and into quiescent surroundings have been developed. These expressions were obtained by using a modified Laplace transform to solve the linearized potential flow equation. The initial slope of the jet boundary was kept as a parameter in the final expressions, which permitted a study of the use of an exact, in place of a linearized, initial value. Results were compared with characteristics solutions and experimental data.

An expression was also developed to determine the pressure field of a supersonic stream surrounding the jet. This expression was applied to determine the pressure influence of the jet on a nearby flat plate. These results were also compared with experimental data.

INTRODUCTION

Various flight vehicles have jets issuing from their exhaust nozzles near other components such as wings, control surfaces, and other engines. The contour of the jet and resulting field about it may then alter the pressure distribution on these nearby components and thus their performance (refs. 1 to 3). The pluming jet from an underexpanded nozzle may transmit pressure changes upstream on the boattail surface through the boundary layer and even cause flow separation (ref. 4). The initial expansion of the jet also influences the downstream mixing region. Initial-jet-contour prediction is important for the determination of the pressure on a wide-base annulus (ref. 5).

The number of independent variables involved in the relevant geometries and operating conditions usually precludes completeness of economic systematic experimental solution to these problems. A necessary step toward the quantitative prediction of these effects is a means of determining the initial contour of the exhaust jet. An extensive use of

characteristics is made in references 6 and 7 to determine the initial contour of a supersonic jet exhausting into still air. Replacing the quiescent air by a supersonic stream, however, appreciably increases the labor to solve the already unwieldy problem when using characteristics. A simplified step-by-step method of approximating initial jet contour is presented in reference 8.

A theory which leads to a simple explicit relation for the contour of a jet exhausting into quiescent surroundings is presented in reference 9. This method utilizes the linearized equations of motion, however, and is therefore accompanied by questions of accuracy and range of applicability. The predominant feature of this method is that of taking the Laplace transform of the linearized supersonic equations of motion. Piecewise continuous flows such as found in the periodic structure of jets exhausting into still air then become continuous in the transformed plane. Advantage is also gained by the supersonic potential equation for axisymmetric flow reducing to an ordinary differential equation in the transformed plane. Essentially this same technique was used in the work of reference 10 to study the oscillations of a supersonic jet exhausting into a supersonic ambient stream. Although limited in quantitative application, this analysis contributes appreciably to an understanding of the role of various variables in determining jet contour.

This paper extends the method of reference 9 to the case of an axisymmetric jet exhausting into a supersonic stream. The inverse Laplace transforms of the internal (jet) flow and external (ambient) flow were taken separately in this report and then combined in the physical plane to find the jet boundary as opposed to the taking of the inverse transform in the last step in reference 10. The initial inclination of the jet was preserved as a separate parameter in the final equation for jet contour so that improvement of linearized results by exact initial conditions could be studied. Isolation of the initial inclination then also provides a means of semiempirically accounting for effects of nozzle wall and boattail angle. The method was finally extended to determine the pressure field about the jet in the external supersonic stream for purposes of determining jet influences on nearby aerodynamic surfaces.

SYMBOLS

a	constant in eq. (2)
a_1, a_2, a_3, a_4, a_5	constants in eq. (9)
β	$\sqrt{M^2 - 1}$

b	constant in eq. (2)
b_1, b_2, b_3	constant coefficients in differential eqs. used to determine R
H	Heaviside unit function, $H(z) = 0$ for $z < 0$ and $H(z) = 1$ for $z > 0$
I_n	modified Bessel function of first kind of order n
K_n	modified Bessel function of second kind of order n
k	constant in eq. (11b)
$\mathscr{L}$	modified Laplace transform such as $\mathscr{L}\{f(z)\} = \lambda \int_0^z f(z)e^{-\lambda z}\, dz$
M	Mach number
p	pressure
q_1, q_2	constants used in conjunction with eq. (12)
R	$r - r_0$
r	radial distance from jet axis of symmetry
s	dummy variable
U	undisturbed velocity in z-direction
z	axial distance from nozzle-exit station
α, β	constants in eq. (12)
γ	ratio of specific heats
δ	Dirac delta function, $\delta(z) = 0$ for $z \neq 0$ and $\delta(z) = \infty$ for $z = 0$ and $\int_{-\infty}^{\infty} \delta(z)dz = 1$
η	slope of jet boundary
λ	variable in transformed space
ν_1, ν_2, ν_3	constants in second-order solution of eq. (9)
ξ_1, ξ_2, ξ_3	roots of cubic characteristics equation

ρ mass density

ψ perturbation velocity potential due to jet

Subscripts:

a quiescent medium surrounding jet

b boundary of jet

ext external

int internal

j undisturbed conditions in jet at nozzle exit

0 boundary of jet at nozzle exit

∞ undisturbed external stream

Superscripts:

' differentiation with respect to argument of function

$\bar{}$ operational form

ANALYSIS

Two cases are considered: an axisymmetric supersonic jet exhausting into a supersonic stream (case 1) and into a quiescent medium (case 2). In the linearized theory, the internal flow (from the nozzle) and external flow are both assumed to be uniform and parallel to one another at the nozzle-exit station (fig. 1). It is also assumed for case 1 that no appreciable base region is present; however, for a very large base, case 1 reduces to case 2. Simple explicit algebraic expressions are derived for the jet contour for both of these cases. An expression which can be evaluated by quadratures to determine the pressure field in the supersonic stream about the jet is also derived. These equations and their restrictions are listed in the SUMMARY OF RESULTS for convenient reference.

Basic Equations

Let the jet axis coincide with the z-axis in a cylindrical coordinate system and let the nozzle-exit station be at $z = 0$. The familiar linearized supersonic potential equation based on continuity, momentum, and irrotationality considerations is for axisymmetric flow

$$\frac{\partial^2\varphi}{\partial r^2} + \frac{1}{r}\frac{\partial\varphi}{\partial r} - B^2\frac{\partial^2\varphi}{\partial z^2} = 0$$

where φ is the perturbation velocity potential due to the jet, and $B = \sqrt{M^2 - 1}$. No disturbance from the jet is propagated ahead of the nozzle-exit station, and thus $(\partial\varphi/\partial z)_{z=0} = \varphi(0) = 0$. Following the procedure of reference 9, the potential equation is transformed into operational form by multiplying by $\lambda e^{-\lambda z}$ and then integrating with respect to z between the limits 0 to ∞. This results in the Bessel equation

$$\frac{d^2\bar{\varphi}}{dr^2} + \frac{1}{r}\frac{d\bar{\varphi}}{dr} - B^2\lambda^2\bar{\varphi} = 0 \tag{1}$$

where a bar over a symbol signifies that it is in transformed space as opposed to the original space, that is,

$$\bar{f}(\lambda) = \lambda\int_0^\infty f(z)e^{-\lambda z}\,dz$$

The general solution of equation (1) is

$$\bar{\varphi} = aK_0(Br\lambda) + bI_0(Br\lambda) \tag{2}$$

Boundary conditions. - Let $\eta(z)$ be the slope of the jet boundary, and let the subscript b denote conditions on this boundary between the internal (jet) and external flow. No mixing is considered.

The boundary conditions to be satisfied by both internal and external streams are

$$\left(\frac{\partial\varphi}{\partial r}\right)_b = U\eta(z) \tag{3a}$$

$$p_{b_{ext}} = p_{b_{int}} \tag{3b}$$

The external flow must also satisfy the boundary condition

$$\left.\begin{aligned} &\frac{\partial\varphi}{\partial z} \to 0 \quad \text{as} \quad r \to \infty \\ &\text{or in transformed space} \\ &\lambda\bar{\varphi} \to 0 \quad \text{as} \quad r \to \infty \end{aligned}\right\} \tag{4a}$$

whereas the internal flow must satisfy

$$\left.\begin{aligned} &\frac{\partial\varphi}{\partial r} = 0 \quad \text{at} \quad r = 0 \\ &\text{or in transformed space} \\ &\frac{\partial\bar{\varphi}}{\partial r} = 0 \quad \text{at} \quad r = 0 \end{aligned}\right\} \tag{4b}$$

The last two boundary conditions are satisfied by setting $a = 0$ in equation (2) for internal flow and $b = 0$ for external flow. This is apparent from the variation of the Bessel functions K_n and I_n with their arguments.

External flow. - Use of equations (2), (3a), and (4a) determines a as

$$a = - \frac{U_\infty \bar{\eta}(\lambda)}{B_\infty \lambda K_1(B_\infty r_b \lambda)}$$

so that

$$\bar{\varphi} = - \frac{U_\infty \bar{\eta}(\lambda) K_0(B_\infty r \lambda)}{B_\infty \lambda K_1(B_\infty r_b \lambda)}$$

where the subscript ∞ refers to undisturbed conditions in the external flow.

The linearized pressure coefficient

$$\frac{c_p}{2} = \frac{p - p_\infty}{\rho_\infty U_\infty^2} = - \frac{1}{U_\infty} \frac{\partial \varphi}{\partial z}$$

in operational form becomes

$$\frac{\bar{p} - p_\infty}{\rho_\infty U_\infty^2} = - \frac{\lambda \bar{\varphi}}{U_\infty} \tag{5}$$

so that

$$\frac{\bar{p} - p_\infty}{\rho_\infty U_\infty^2} = \frac{\bar{\eta}(\lambda) K_0(B_\infty r \lambda)}{B_\infty K_1(B_\infty r_b \lambda)} \tag{6}$$

Internal flow. - Combining equations (2), (3a), and (4b) determines b as

$$b = \frac{U_j \bar{\eta}(\lambda)}{B_j \lambda I_1(B_j \lambda r_b)}$$

and thus

$$\bar{\varphi} = \frac{U_j \bar{\eta}(\lambda) I_0(B_j \lambda r)}{B_j \lambda I_1(B_j \lambda r_b)}$$

where the subscript j refers to jet flow conditions at the nozzle-exit station (z = 0). The linearized pressure coefficient in operational form then becomes

$$\frac{\overline{p} - p_j}{\rho_j U_j^2} = - \frac{\overline{\eta}(\lambda) I_0(B_j \lambda r)}{B_j I_1(B_j \lambda r_b)} \tag{7}$$

Jet Contour for Supersonic External Flow

Substitution of equations (3b), (6), and (7) in the identity

$$\frac{\overline{p}_b - p_j}{\rho_j U_j^2} = \left(\frac{\overline{p}_b - p_\infty}{\rho_\infty U_\infty^2} + \frac{p_\infty - p_j}{\rho_\infty U_\infty^2} \right) \frac{\rho_\infty}{\rho_j} \frac{U_\infty^2}{U_j^2}$$

results in

$$\frac{p_j - p_\infty}{\rho_j U_j^2} = \frac{\rho_\infty U_\infty^2}{\rho_j U_j^2} \frac{\overline{\eta}(\lambda)}{B_\infty} \frac{K_0(B_\infty r_b \lambda)}{K_1(B_\infty r_b \lambda)} + \frac{\overline{\eta}(\lambda)}{B_j} \frac{I_0(B_j r_b \lambda)}{I_1(B_j r_b \lambda)} \tag{8}$$

The interpretation of equation (8) into physical space is quite lengthy and is given in the appendix. This appendix contains essentially the same expressions as interpreted in reference 9 but is included here for completeness. The result is that

$$\frac{p_j - p_\infty}{\rho_j U_j^2} = a_1 \eta(z) - \frac{a_2}{2 r_b} \int_0^z \eta(s)\, ds + \frac{3}{8} \frac{a_3}{r_b} \int_0^z \left(\frac{z - s}{B_j r_b} \right) \eta(s)\, ds$$

$$- \frac{3}{16} \frac{a_4}{r_b} \int_0^z \left(\frac{z - s}{B_j r_b} \right)^2 \eta(s)\, ds + \frac{21}{256} \frac{a_5}{r_b} \int_0^z \left(\frac{z - s}{B_j r_b} \right)^3 \eta(s)\, ds + \ldots \tag{9}$$

for $0 \leq \frac{z}{B_j r_b} < 2$

where

$$a_1 = \frac{\rho_\infty U_\infty^2}{\rho_j U_j^2} \frac{1}{B_\infty} + \frac{1}{B_j}$$

$$a_2 = \frac{\rho_\infty U_\infty^2}{\rho_j U_j^2} \frac{1}{B_\infty^2} - \frac{1}{B_j^2}$$

$$a_3 = \frac{\rho_\infty U_\infty^2}{\rho_j U_j^2} \frac{B_j}{B_\infty^3} + \frac{1}{B_j^2}$$

$$a_4 = \frac{\rho_\infty U_\infty^2}{\rho_j U_j^2} \frac{B_j^2}{B_\infty^4} - \frac{1}{B_j^2}$$

$$a_5 = \frac{\rho_\infty U_\infty^2}{\rho_j U_j^2} \frac{B_j^3}{B_\infty^5} + \frac{1}{B_j^2}$$

First-order solution. - Consider first the solution of equation (9) in which powers of $(z - s)/B_j r_b$ greater than the first are neglected. Call this the "first-order" solution. Assume that changes in r_b are small compared with the radius of the jet at the nozzle-exit station r_0, so that $r_b \approx r_0$. Then differentiating equation (9) with respect to z results in the differential equation

$$\frac{d^2 R_b}{dz^2} + b_1 \frac{dR_b}{dz} + b_2 R_b = 0$$

where

$$R_b = r_b - r_0 = \int_0^z \eta(s)\, ds$$

$$b_1 = - \frac{a_2}{2 r_0 a_1}$$

$$b_2 = \frac{3}{8} \frac{a_3}{B_j r_0^2 a_1}$$

The boundary conditions are

$$R(0) = 0$$

and

$$\left(\frac{dR}{dz}\right)_{z=0} = \eta(0)$$

From equation (9)

$$\eta(0) = \frac{p_j - p_\infty}{\rho_j U_j^2 a_1} = \frac{1 - \frac{p_\infty}{p_j}}{\gamma_j M_j^2 a_1} \tag{10}$$

The first-order solution is then

$$R_b = - \frac{\eta(0)\left(e^{-\sqrt{\frac{b_1^2}{4} - b_2}\, z} - e^{\sqrt{\frac{b_1^2}{4} - b_2}\, z}\right)}{2e^{b_1 z/2}\sqrt{\frac{b_1^2}{4} - b_2}} \tag{11a}$$

For the usual case, $b_2 > b_1^2/4$, and hence the exponents of e in the numerator are conjugate imaginary numbers. In this case the solution reduces to

$$R_b = \frac{\eta(0)\, \sin\,(kz)}{ke^{b_1 z/2}} \tag{11b}$$

where $k = \sqrt{b_2 - b_1^2/4}$.

Second-order solution. - Consider next the solution of equation (9) in which only powers of $(z - s)/B_j r_b$ greater than the second are neglected. Call this the "second-order" solution. For $r \approx r_0$ the second derivative of equation (9) with respect to z results in the differential equation

$$\frac{d^3 R_b}{dz^3} + b_1 \frac{d^2 R_b}{dz^2} + b_2 \frac{dR_b}{dz} + b_3 R = 0$$

where b_1 and b_2 are the same as before, and

$$b_3 = - \frac{3}{8} \frac{a_4}{r_0^3 B_j^2 a_1}$$

The boundary condition

$$\eta'(0) = \frac{a_2}{2r_0 a_1} \eta(0)$$

is obtained from the first derivative of equation (9). This supplements the two previous boundary conditions.

From a source such as reference 11

$$R_b = \nu_1 e^{\xi_1 z} + \nu_2 e^{\xi_2 z} + \nu_3 e^{\xi_3 z}$$

where ξ_1, ξ_2, and ξ_3 are roots of the algebraic equation

$$\xi^3 + b_1\xi^2 + b_2\xi + b_3 = 0$$

In cases of practical interest ξ_1, ξ_2, and ξ_3 are unequal; ξ_1 can be a real number, and ξ_2 and ξ_3 are complex conjugate. It then follows that ν_1 is real and ν_2 is a complex conjugate with ν_3. Evaluation of the ν's from the boundary conditions then results in

$$\nu_1 = \frac{\eta(0)\xi_1}{(\xi_1 - \xi_3)(\xi_1 - \xi_2)}$$

$$\nu_2 = -\frac{\eta(0)\xi_2}{(\xi_1 - \xi_2)(\xi_2 - \xi_3)}$$

$$\nu_3 = \frac{\eta(0)\xi_3}{(\xi_1 - \xi_3)(\xi_2 - \xi_3)}$$

The solution for R then reduces to

$$R_b = \frac{\eta(0)}{3(\alpha^2 + \alpha\beta + \beta^2)} \left\{ -\left(\alpha + \beta + \frac{b_1}{3}\right) e^{-\left(\alpha+\beta+\frac{b_1}{3}\right)z} \right.$$
$$+ \frac{e^{\left(\frac{\alpha+\beta}{2} - \frac{b_1}{3}\right)z}}{\sqrt{3}\,(\alpha - \beta)} \left(\left[\sqrt{3}\,(\alpha^2 - \beta^2) + \frac{b_1}{\sqrt{3}}\,(\alpha - \beta) \right] \cos\left[\frac{\sqrt{3}}{2}\,(\alpha - \beta)z \right] \right.$$
$$\left. \left. + \left[3(\alpha^2 + \beta^2) - b_1(\alpha + \beta) \right] \sin\left[\frac{\sqrt{3}}{2}\,(\alpha - \beta)z \right] \right) \right\} \qquad (12)$$

if $\frac{q_1^3}{27} + \frac{q_2^2}{4} > 0$, which is the usual case, and where

$$\alpha = \sqrt[3]{\left| -\frac{q_2}{2} + \sqrt{\frac{q_1^3}{27} + \frac{q_2^2}{4}} \right|} \quad \text{if} \quad \frac{q_1^3}{27} < 0$$

$$= -\sqrt[3]{\left| -\frac{q_2}{2} + \sqrt{\frac{q_1^3}{27} + \frac{q_2^2}{4}} \right|} \quad \text{if} \quad \frac{q_1^3}{27} > 0$$

$$\beta = \sqrt[3]{\left| -\frac{q_2}{2} - \sqrt{\frac{q_1^3}{27} + \frac{q_2^2}{4}} \right|}$$

$$q_1 = b_2 - \frac{b_1^2}{3}$$

$$q_2 = b_3 - \frac{b_1 b_2}{3} + \frac{2b_1^3}{27}$$

Jet Contour for Quiescent Surroundings

The following derivation is essentially that of reference 9 except that the answer is given as a series expression and the initial slope of the jet contour is labeled.

At the boundary of the jet the pressure must equal the constant value of the quiescent external field, and

$$\frac{p_a - p_j}{\rho_j U_j} = -\lambda b I_0(B_j r_b \lambda)$$

by use of equations (2), (4b), and (5), the undisturbed or reference stream now being the flow at the nozzle-exit station. The subscript a refers to the quiescent external field. Solving for b and using equation (2) again yield

$$\bar{\varphi} = \frac{p_j - p_a}{\rho_j U_j} \frac{I_0(B_j r \lambda)}{\lambda I_0(B_j r_b \lambda)}$$

At the jet boundary

$$\bar{\eta}(\lambda) = \frac{1}{U_j}\left(\frac{\partial \bar{\varphi}}{\partial r}\right)_b = \frac{p_j - p_a}{\rho_j U_j^2} B_j \frac{I_1(B_j r_0 \lambda)}{I_0(B_j r_0 \lambda)} \tag{13}$$

if $r_b \approx r_0$. It then follows that

$$R_b = \int_0^z \eta(z)dz = \frac{p_j - p_a}{\rho_j U_j^2} B_j^2 r_0 \int_0^{z/B_j r_0} \mathcal{L}^{-1}\left\{\frac{I_1(B_j r_0 \lambda)}{I_0(B_j r_0 \lambda)}\right\} d\left(\frac{z}{B_j r_0}\right)$$

Using equations (A2) for the Bessel functions and dividing the numerator by the denominator result in

$$R_b = \frac{p_j - p_a}{\rho_j U_j^2} B_j^2 r_0 \int_0^{z/B_j r_0} \mathcal{L}^{-1}\left\{1 - \frac{1}{2B_j r_0 \lambda} - \frac{1}{8(B_j r_0 \lambda)^2} - \frac{1}{8(B_j r_0 \lambda)^3}\right.$$

$$\left. - \frac{25}{128(B_j r_0 \lambda)^4} - \cdots\right\} d\left(\frac{z}{B_j r_0}\right) = \frac{p_j - p_a}{\rho_j U_j^2} B_j^2 r_0 \left[\frac{z}{B_j r_0} - \frac{1}{4}\left(\frac{z}{B_j r_0}\right)^2\right.$$

$$\left. - \frac{1}{48}\left(\frac{z}{B_j r_0}\right)^3 - \frac{1}{192}\left(\frac{z}{B_j r_0}\right)^4 - \cdots\right]$$

The flow in the immediate vicinity of the nozzle trailing edge is two-dimensional, since $\lim_{z \to 0} \frac{r_b - r_0}{r_0} = 0$. For two-dimensional flow

$$\frac{p_j - p_a}{\rho_j U_j^2} B_j = \eta(0) \tag{14}$$

so that

$$\frac{R_b}{r_0} = \eta(0)\, B_j \left[\frac{z}{B_j r_0} - \frac{1}{4}\left(\frac{z}{B_j r_0}\right)^2 - \frac{1}{48}\left(\frac{z}{B_j r_0}\right)^3 - \frac{1}{192}\left(\frac{z}{B_j r_0}\right)^4 - \cdots\right] \tag{15}$$

Comparison of this result with the numerical result of reference 9 is shown in figure 2. Good agreement is obtained up to a $z/B_j r_0$ of almost 2.

Pressure Field of External Supersonic Flow

An expression to determine the incremental pressure due to the influence of the jet on the external supersonic field is derived in this section. This expression may be useful in determining jet interferences with forces and moments on flight configurations having surfaces within the characteristic surface of disturbance emanating from the nozzle-exit station. Some application is shown in the section DISCUSSION OF RESULTS.

Proceeding to interpret equation (6), for $r_b \approx r_0$,

$$\frac{p - p_\infty}{\rho_\infty U_\infty^2} = \mathcal{L}^{-1}\left\{\frac{\bar{\eta}(\lambda)K_0(B_\infty r\lambda)}{B_\infty K_1(B_\infty r_0\lambda)}\right\}$$

$$= \frac{1}{B_\infty}\int_0^z S(z - s)\eta(s)ds \qquad (16)$$

by use of the convolution equation where

$$\bar{S}(\lambda) = \frac{\lambda K_0(B_\infty r\lambda)}{K_1(B_\infty r_0\lambda)}$$

Using equation (A1)

$$\bar{S}(\lambda) = \lambda\sqrt{\frac{r_0}{r}}\, e^{-B_\infty\lambda R}\left[\frac{1 + \sum_{m=1}^{\infty}\frac{(0,m)}{(2Br\lambda)^m}}{1 + \sum_{m=1}^{\infty}\frac{(1,m)}{(2Br\lambda)^m}}\right]$$

$$= \lambda\sqrt{\frac{r_0}{r}}\, e^{-B_\infty\lambda R}\,\bar{Q}$$

where

$$\bar{Q} = \frac{1 - \frac{1}{8B_\infty\lambda r} + \frac{9}{128(B_\infty\lambda r)^2} - \frac{75}{1024(B_\infty\lambda r)^3} + \frac{3675}{32,768(B_\infty\lambda r)^4} + \cdots}{1 + \frac{3}{8B_\infty\lambda r_0} - \frac{15}{128(B_\infty\lambda r_0)^2} + \frac{105}{1024(B_\infty\lambda r_0)^3} - \frac{4725}{32,768(B_\infty\lambda r_0)^4} + \cdots}$$

Consider the variation of $\bar{Q}$ with $1/r$. This power series can be expanded into a convergent Taylor series about r_0 for constant B_∞ and λ as

$$\bar{Q}(r) = \bar{Q}(r_0) + \bar{Q}'(r_0)\frac{R}{1!} + \bar{Q}''(r_0)\frac{R^2}{2!} + \cdots$$

The coefficients can be evaluated as follows:

$$\bar{Q}(r_0) = 1 - \frac{1}{2B_\infty\lambda r_0} + \frac{3}{8(B_\infty\lambda r_0)^2} - \frac{3}{8(B_\infty\lambda r_0)^3} + \frac{63}{128(B_\infty\lambda r_0)^4} + \cdots$$

$$\overline{Q}'(r_0) = \frac{1}{8B_\infty \lambda r_0^2} - \frac{3}{16B_\infty^2 \lambda^2 r_0^3} + \frac{39}{128B_\infty^3 \lambda^3 r_0^4} - \frac{153}{256B_\infty^4 \lambda^4 r_0^5} + \cdots$$

$$\overline{Q}''(r_0) = -\frac{1}{4B_\infty \lambda r_0^3} + \frac{33}{64B_\infty^2 \lambda^2 r_0^4} - \frac{141}{128B_\infty^3 \lambda^3 r_0^5} + \frac{351}{128B_\infty^4 \lambda^4 r_0^6} + \cdots$$

and so forth, so that

$$\overline{S}(\lambda) = \lambda\sqrt{\frac{r_0}{r}}\, e^{-B_\infty \lambda R}\left[1 - \frac{1}{2B_\infty r_0 \lambda} + \frac{3}{8(B_\infty r_0 \lambda)^2} - \frac{3}{8(B_\infty r_0 \lambda)^3} + \frac{63}{128(B_\infty r_0 \lambda)^4}\right.$$
$$+ \left(\frac{1}{8B_\infty \lambda r_0^2} - \frac{3}{16B_\infty^2 \lambda^2 r_0^3} + \frac{39}{128B_\infty^3 \lambda^3 r_0^4} - \frac{153}{256B_\infty^4 \lambda^4 r_0^5}\right) R$$
$$\left. + \left(-\frac{1}{4B_\infty \lambda r_0^3} + \frac{33}{64B_\infty^2 \lambda^2 r_0^4} - \frac{141}{128B_\infty^3 \lambda^3 r_0^5} + \frac{351}{128B_\infty^4 \lambda^4 r_0^6}\right)\frac{R^2}{2} + \cdots\right]$$

Collecting terms containing like powers of λ and taking the inverse transform of $\overline{S}(\lambda)$ yield

$$S(z) = \sqrt{\frac{r_0}{r}}\left[\delta(z - B_\infty R) - \frac{1}{2B_\infty}\left(\frac{1}{r_0} - \frac{R}{4r_0^2} + \frac{R^2}{4r_0^3}\right) H(z - B_\infty R)\right.$$
$$+ \frac{1}{8B_\infty^2}\left(\frac{3}{r_0^2} - \frac{3R}{2r_0^3} + \frac{33R^2}{16r_0^4}\right)(z - B_\infty R) H(z - B_\infty R)$$
$$- \frac{1}{16B_\infty^3}\left(\frac{3}{r_0^3} - \frac{39R}{16r_0^4} + \frac{141R^2}{32r_0^5}\right)(z - B_\infty R)^2 H(z - B_\infty R)$$
$$\left. + \frac{1}{768B_\infty^4}\left(\frac{63}{r_0^4} - \frac{153R}{2r_0^5} + \frac{351R^2}{r_0^6}\right)(z - R_\infty R)^3 H(z - B_\infty R) + \cdots\right] \qquad (17)$$

where δ is the Dirac delta function and H is the Heaviside unit function. The series in equation (17) converges for $0 < z - B_\infty R < B_\infty r_0$ and $R \ll r_0$. Finally substituting equation (17) in (16) yields the following expression for pressure coefficient:

$$\frac{p - p_\infty}{\rho_\infty U_\infty^2} = \frac{1}{B_\infty}\sqrt{\frac{r_0}{r}}\left[\eta(z - B_\infty R) - \frac{1}{2B_\infty}\left(\frac{1}{r_0} - \frac{R}{4r_0^2} + \frac{R^2}{4r_0^3}\right)\int_0^{z-B_\infty R}\eta(s)ds\right.$$

$$+ \frac{1}{8B_\infty^2}\left(\frac{3}{r_0^2} - \frac{3R}{2r_0^3} + \frac{33R^2}{16r_0^4}\right)\int_0^{z-B_\infty R}(z - s - B_\infty R)\eta(s)ds$$

$$- \frac{1}{16B_\infty^3}\left(\frac{3}{r_0^3} - \frac{39R}{16r_0^4} + \frac{141R^2}{32r_0^5}\right)\int_0^{z-B_\infty R}(z - s - B_\infty R)^2\eta(s)ds$$

$$\left.+ \frac{1}{768B_\infty^4}\left(\frac{63}{r_0^4} - \frac{153R}{2r_0^5} + \frac{351R^2}{r_0^6}\right)\int_0^{z-B_\infty R}(z - s - B_\infty R)^3\eta(s)ds + \ldots\right] \quad (18)$$

The slope at the jet boundary $\eta(z)$ may be obtained by differentiating equations (11) or (12) with respect to z or by solving equation (9) directly for the slope by the procedure used previously to obtain R.

DISCUSSION OF RESULTS

The equations for jet contour for a supersonic external field (eqs. (11) and (12)) as well as a quiescent external field (eq. (15)) each comprise essentially two separable parts: (1) a term denoting the initial slope of the jet boundary ($\eta(0)$) and (2) the remaining part of the equation, which determines the shape or curvature of the jet boundary as a function of axial distance from the nozzle exit. Comparisons can readily be made between the jet shapes determined by equations (11) and (12) and between the linearized and exact initial jet boundary $\eta(0)$. Comparisons of the operational theory in general with characteristic and experimental data are less systematic because of the limited amount of these data available. In most cases air with a specific-heat ratio of 1.4 was used as the working medium for both internal and external flows. Any compressible fluids for which average specific heats and molecular weights can be selected, however, should be amenable to the theory.

Jet Contour for Supersonic External Flow

Equation (11) for jet contour is based on a solution of equation (9) in which all powers of $z/B_\infty r_b$ greater than the first are assumed negligible in the series expressions for W and T' (eqs. (A5) and (A7)),

whereas in the derivation of equation (12) powers of $z/B_\infty r_b$ greater than the second are neglected. The solutions were, therefore, respectively labeled the first- and second-order solutions of the jet-contour equation. In either case the series representations of W and T' are valid only for small $z/B_\infty r_b$ and $z/B_j r_b$ less than 2.

Jet shape. - Figure 3 shows comparisons of the results of equations (11) and (12) over a range of internal and external Mach numbers of 2 to 9 and at nozzle-exit to free-stream static-pressure ratios of 2/3 to 5. The linearized value of $\eta(0)$ was arbitrarily used for this figure; however, it enters into equations (11) and (12) only as a multiplier and, therefore, only results as a scale effect on the abscissa.

Over the range of Mach numbers investigated very close agreement between the two solutions was obtained for axial distances from the nozzle exit of $0 \leq z/Br_0 \leq 1$. As axial distance is further increased, the first-order solution predicts an increasingly greater jet-contour radius than the second-order solution for $p_j/p_\infty \neq 1$. The greatest difference in results, however, is less than 4 percent. This close agreement should, in turn, justify utilization of the simplicity of equations (11) over (12) for practical cases of determining jet shape.

Initial slope of jet boundary. - A comparison of the linearized and exact results for $\eta(0)$ is shown in figure 4 over the same ranges of Mach number and pressure ratio as in figure 3. The exact results were obtained by use of Prandtl-Meyer expansion curves for the expanding flow on one side of the jet boundary and by use of two-dimensional shock charts on the compression side of the boundary. A unique solution for $\eta(0)$ is obtained which yields continuity of pressure and velocity direction across the jet boundary.

Beyond the common intersection at (1,0) the curves of figure 4 reach a limited deviation and then a second intersection point as pressure ratio is increased. Beyond the second intersection point a deviation greater than 50 percent was reached at the highest jet and lowest stream Mach numbers. As M_∞ increases and M_j decreases, the second intersection point is located at higher p_j/p_∞, and deviation of the linear expression from the exact is less pronounced.

The two-dimensional shock-expansion wave procedure of determining $\eta(0)$ provides a means of accounting for local deviations in flow direction due to nozzle wall and boattail angles. Although this procedure is justified locally, that is, near the nozzle trailing edge, the combination of this $\eta(0)$ with a linearized shape parameter for uniform axial initial flows may be labeled semiempirical and is studied in figures 5 and 6.

Comparison with experimental and characteristics data. - Some results of using the first-order solution in conjunction with the exact initial slope are shown in figure 5 for three geometries and test conditions (refs. 3, 6, and 8). The external flow was uniform and approached the jet in the direction of the jet axis in references 3 and 8; however, the external flow passed over a boattail and approached the jet at an angle of 9° in reference 6. In all three references the internal flow left the nozzle at directions other than axial, the nozzle wall angles being 12° for reference 3 and 12.5° for references 6 and 8. These angles were, however, easily accounted for locally in the two-dimensional shock-expansion procedure discussed in the last section.

A comparison of the operational theory with the experimental data of reference 3 is shown in figure 5(a). Results are within the indicated mixing zone of the internal and external streams. The mixing zone is obtained from a schlieren photograph of the jet interaction region.

Comparisons with two characteristics calculations of references 6 and 8 are presented in figures 5(b) and (c). Exact values for the initial slope of the jet were used in both calculations; hence the curves start out together. At distances farther from the nozzle exit the operational theory curve was slightly below that of the characteristics theory, the maximum deviation being less than 10 percent. Use of the results of figure 3 shows that the "first-order" solution is slightly closer to the characteristics curves than the "second-order" solution.

Jet Contour for Quiescent Surroundings

Again the two-dimensional expression may be used for the initial slope. Only a curve of the Prandtl-Meyer relation or a shock chart is needed to determine $\eta(0)$, depending on whether the nozzle is underexpanded or overexpanded as long as the nozzle is flowing full, that is, the flow is not separated. A number of initial slopes for a jet expanding in quiescent air are presented in reference 7 for various specific-heat ratios and for static-pressure ratios up to 12 and supersonic jet Mach numbers up to 3.

A comparison of the linearized equation (eq. (14)) with exact initial slopes is shown in figure 7. At low pressure ratios the agreement between linearized and exact values is good, but it becomes poor rapidly as pressure ratio is increased. At a pressure ratio of 5 the exact value is almost twice the linearized. This result together with that of figure 4 shows that considerable improvement can be made by using exact $\eta(0)$ as pressure ratio is increased and external Mach number is decreased.

A number of jet contours determined by equation (15) and an exact $\eta(0)$ are compared with characteristics-determined contours of references

6, 7, and 12 in figure 6. The change in jet boundary due to changes in $\eta(0)$ is predicted within 12 percent in figures 6(a) and (b). The main difference between the operational theory and characteristics contours shown in figures 6(a) and (b) is due to a shifting of the axial position of jet maximum diameter with pressure ratio which is not produced by the operational theory. Deviation between the two calculations is, of course, zero at the nozzle exit. The maximum deviation in figures 6(a) and (b) is less than 23 percent. Figure 6(c) presents results computed at extremely high pressure ratios but only over a range of axial distance of $0 \leq \frac{z}{B_j r_0} \leq 1$. Agreement was within 10 percent.

Pressure Field of External Supersonic Flow

An example is worked to determine the jet incremental pressure on a flat surface, the closest distance of which from the jet axis is a straight line located 1 nozzle-exit diameter away from and parallel to the nozzle axis. The pressures on this surface are the same as those on a reflection plane located midway between two identical and parallel jets. The zone of influence of the jet in this plane starts a distance of $B_\infty(r - r_0)$ downstream of the nozzle-exit station for completely linearized flow (for an exact $\eta(0)$ the disturbance starts somewhat upstream). A reflected wave from this location does not influence the jet for an additional distance of approximately $B_\infty(r - r_0)$. Therefore the jet contour remains independent of the external surface for approximately $2B(r - r_0)$ downstream of the nozzle-exit station. The boundary condition on the flat surface is that the component of velocity normal to the surface is zero. This is automatically satisfied. The pressure on this surface in the region $1 \leq \frac{z}{B_\infty(r - r_0)} \leq 3$ is simply twice that given by equation (18) in space, since the pressure from the two jets can be added together because of the linearity of the external field.

Computations of pressure coefficient on this surface were made for undisturbed external Mach numbers of 2.5 and 3. Comparison is made in figure 8 with the experimental data of reference 3 on the line of intersection of the aerodynamic surface with the plane passing through the axes of both the real and the hypothetical jet. The derivative of the first-order solution (eq. (11b)) with the exact initial jet slope was used to determine η for use in equation (18). The integrals in equation (18) were then evaluated numerically. The location where the outgoing waves hit the aerodynamic surface was adjusted forward to the position consistent with the determination of $\eta(0)$.

In general, fair agreement was obtained between the theoretical and experimental values of pressure coefficient. The initial pressure rise

on the surface is gradual in the actual case instead of abrupt, probably because of the influence of the boundary layer. Some differences may be due to an unaccounted for curvature in a plane normal to the jet centerline of the surface used to get the experimental data.

Effects of additional geometries can be determined by superposition of the corresponding linearized flow fields as long as the equation describing the boundary condition can be made linear.

SUMMARY OF RESULTS

The following equations were derived to determine the radius r_b of a supersonic jet as a function of axial distance z from the nozzle-exit station and to determine the pressure field about the jet.

1. For a jet exhausting into a supersonic stream and with the nozzle axis parallel to the undisturbed external stream

$$r_b = r_0 - \frac{\left(\eta(0)e^{-\sqrt{\frac{b_1^2}{4} - b_2}\, z} - e^{\sqrt{\frac{b_1^2}{4} - b_2}\, z}\right)}{2\sqrt{\frac{b_1^2}{4} - b_2}\, e^{b_1 z/2}} \qquad 0 \le \frac{z}{B_j r_0}, \frac{z}{B_\infty r_0} < 2$$

where $\eta(0)$ is the initial slope of the free jet boundary at the nozzle exit, r_0 is the radius of the nozzle at its exit station, b_1 and b_2 are constants depending only on the undisturbed flow inside the nozzle at its exit station and on the undisturbed external stream (these constants are described on p. 8), and

$$B_j = \sqrt{M_j^2 - 1}$$

$$B_\infty = \sqrt{M_\infty^2 - 1}$$

M_j and M_∞ are the Mach numbers of the undisturbed flows inside the nozzle at its exit station and in the external stream, respectively. For the usual case, $b_2 > b_1^2/4$ and this equation can be written as

$$r_b = r_0 + \frac{\eta(0)\, \sin(kz)}{k e^{b_1 z/2}} \qquad 0 < \frac{z}{B_j r_0}, \frac{z}{B_\infty r_0} < 2$$

where

$$k = \sqrt{b_2 - \frac{b_1^2}{4}}$$

A solution for this same problem was also obtained when including one more term in a series expansion before solving the corresponding differential equation to obtain jet contour. The result was again an explicit algebraic equation for jet radius as a function of axial distance from the nozzle-exit station. The equation, however, involved considerably more terms to compute. Differences in results due to including the extra term were less than 4 percent over the range investigated, the simpler solution being slightly closer to the characteristics curves used to check results. The difference between the simpler solution and characteristics and experimental data was within 10 percent over the range investigated.

2. For a jet exhausting into a quiescent surrounding (i.e., a constant-pressure, zero-velocity field)

$$r_b = r_0 + \eta(0) B_j r_0 \left[\frac{z}{B_j r_0} - \frac{1}{4}\left(\frac{z}{B_j r_0}\right)^2 - \frac{1}{48}\left(\frac{z}{B_j r_0}\right)^3 - \frac{1}{192}\left(\frac{z}{B_j r_0}\right)^4 - \cdots \right]$$

$$0 \leq \frac{z}{B_j r_0} < 2$$

The use of an exact initial jet slope obtained from two-dimensional shock and expansion charts in place of a linearized value in any of the preceding equations permits an estimation of the effects of nozzle wall and boattail angles on jet contour. Agreement of the theory was then within 23 percent with two families of characteristics solutions for a nozzle of varying wall angles and exhausting into quiescent air.

Use of an exact $\eta(0)$ in place of linearized values also appreciably improves results at high pressure ratios and low external Mach numbers.

3. The pressure coefficient $(p - p_\infty)/\rho_\infty U_\infty^2$ in the supersonic stream surrounding the jet is given by

$$\frac{p - p_\infty}{\rho_\infty U_\infty^2} = \frac{1}{B_\infty}\sqrt{\frac{r_0}{r}}\left[\eta(z - B_\infty R) - \frac{1}{2B_\infty}\left(\frac{1}{r_0} - \frac{R}{4r_0^2} + \frac{R^2}{4r_0^3}\right)\int_0^{z-B_\infty R}\eta(s)\,ds\right.$$

$$+ \frac{1}{8B_\infty^2}\left(\frac{3}{r_0^2} - \frac{3R}{2r_0^3} + \frac{33R^2}{16r_0^4}\right)\int_0^{z-B_\infty R}(z - s - B_\infty R)\eta(s)\,ds$$

$$- \frac{1}{16B_\infty^3}\left(\frac{3}{r_0^3} - \frac{39R}{16r_0^4} + \frac{141R^2}{32r_0^5}\right)\int_0^{z-B_\infty R}(z - s - B_\infty R)^2\eta(s)\,ds$$

$$\left. + \frac{1}{768B_\infty^4}\left(\frac{63}{r_0^4} - \frac{153R}{2r_0^5} + \frac{351R^2}{r_0^6}\right)\int_0^{z-B_\infty R}(z - s - B_\infty R)^3\eta(s)\,ds + \ldots\right]$$

which converges for $0 < z - B_\infty R < B_\infty r_0$, $R \ll r_0$, and where p_∞, ρ_∞, U_∞, and M_∞ are the pressure, density, velocity, and Mach number of the undisturbed external flow, and s is a dummy variable. The slope $\eta(s)$ of the jet boundary may be obtained by differentiating the contour equation in item 1 with respect to z. This equation was applied to obtain the pressure on a plane surface (such as a wing or tail surface) in the external stream near the jet. The results compared favorably with experimental results.

Lewis Research Center
National Aeronautics and Space Administration
Cleveland, Ohio, February 1, 1960

APPENDIX - INTERPRETATION OF EQUATION (8)

The following equation in operational form is herein interpreted by the procedure of reference 9:

$$\frac{p_j - p_\infty}{\rho_j U_j^2} = \frac{\rho_\infty U_\infty^2}{\rho_j U_j^2} \frac{\overline{\eta}(\lambda)}{B_\infty} \frac{K_0(B_\infty r_b \lambda)}{K_1(B_\infty r_b \lambda)} + \frac{\overline{\eta}(\lambda)}{B_j} \frac{I_0(B_j r_b \lambda)}{I_1(B_j r_b \lambda)} \tag{8}$$

Use is made of the following asymptotic expansions (ref. 13) for the Bessel functions:

$$K(\lambda) \approx \sqrt{\frac{\pi}{2\lambda}}\, e^{-\lambda} \left[1 + \sum_{m=1}^{\infty} \frac{(n,m)}{(2\lambda)^m} \right] \quad \text{for} \quad |\arg \lambda| < \frac{3}{2}\pi \tag{A1}$$

$$I_n(\lambda) \approx \frac{e^{\lambda}}{\sqrt{2\pi\lambda}} \left[1 + \sum_{m=1}^{\infty} (-1)^m \frac{(n,m)}{(2\lambda)^m} \right] + \frac{e^{-\lambda \pm \left(n+\frac{1}{2}\right)\pi i}}{\sqrt{2\pi\lambda}} \left[1 + \sum_{m=1}^{\infty} \frac{(n,m)}{(2\lambda)^m} \right] \quad \text{for} \quad |\arg \lambda \mp \tfrac{1}{2}\pi| < \pi \tag{A2}$$

as $|\lambda| \to \infty$, where

$$(n,m) = \frac{\left(n + m - \frac{1}{2}\right)!}{m!\left(n - m - \frac{1}{2}\right)!}$$

Interpreting the external flow expression first:

$$\mathcal{L}^{-1}\left\{ \frac{\rho_\infty U_\infty^2}{\rho_j U_j^2} \frac{\overline{\eta}(\lambda)}{B_\infty} \frac{K_0(B_\infty r_b \lambda)}{K_1(B_\infty r_b \lambda)} \right\} = \frac{\rho_\infty U_\infty^2}{\rho_j U_j^2} \frac{1}{B_\infty} \mathcal{L}^{-1}\left\{ \frac{\overline{\eta}(\lambda)\lambda \left[1 - \frac{K_1(B_\infty r_b \lambda) - K_0(B_\infty r_b \lambda)}{K_1(B_\infty r_b \lambda)} \right]}{\lambda} \right\}$$

$$= \frac{\rho_\infty U_\infty^2}{\rho_j U_j^2} \frac{1}{B_\infty} \left\{ \eta(z) - \frac{1}{B_\infty r_b} \int_0^z W\left(\frac{z - s}{B_\infty r_b} \right) \eta(s)\, ds \right\} \tag{A3}$$

by use of the convolution equation and where

$$W\left(\frac{z}{B_\infty r_b}\right) = \mathcal{L}^{-1}\left\{\frac{B_\infty r_b \lambda\left[K_1(B_\infty r_b\lambda) - K_0(B_\infty r_b\lambda)\right]}{K_1(B_\infty r_b\lambda)}\right\}$$

Note that the constant $B_\infty r_b$ modifying λ reverts to a reciprocal when modifying z (see e.g. p. 325 of ref. 14). Substituting equations (A1) in the expression for W gives

$$W\left(\frac{z}{B_\infty r_b}\right) = \mathcal{L}^{-1}\left\{B_\infty r_b \lambda\left[1 - \frac{1 + \sum_{m=1}^{\infty} \frac{(0,m)}{(2B_\infty r_b\lambda)^m}}{1 + \sum_{m=1}^{\infty} \frac{(1,m)}{(2B_\infty r_b\lambda)^m}}\right]\right\} \tag{A4}$$

Dividing the numerator by the denominator and interpreting the resulting series term by term yield

$$W\left(\frac{z}{B_\infty r_b}\right) = \frac{1}{2} - \frac{3}{8}\left(\frac{z}{B_\infty r_b}\right) + \frac{3}{16}\left(\frac{z}{B_\infty r_b}\right)^2 - \frac{21}{256}\left(\frac{z}{B_\infty r_b}\right)^3 + \cdots \tag{A5}$$

which converges for small $z/B_\infty r_b$ greater than -2. The remaining internal flow term on the right side of equation (8) is interpreted next.

Let $\eta(z) = \eta(0) + \eta_1(z)$; then

$$\mathcal{L}^{-1}\left\{\frac{\overline{\eta}(\lambda)}{B_j}\frac{I_0(B_j r_b\lambda)}{I_1(B_j r_b\lambda)}\right\} = \frac{1}{B_j}\mathcal{L}^{-1}\left\{\overline{\eta}(\lambda) - \frac{I_1 - I_0}{I_1}\eta(0) - \frac{I_1 - I_0}{\lambda I_1}\lambda\overline{\eta}_1(\lambda)\right\}$$

$$= \frac{1}{B_j}\left\{\eta(z) - \eta(0)\,T\left(\frac{z}{B_j r_b}\right) - \int_0^z \eta_1'(s)\,T\left(\frac{z-s}{B_j r_b}\right)ds\right\}$$

where

$$T\left(\frac{z}{B_j r_b}\right) = \mathcal{L}^{-1}\left\{\frac{I_1(B_j r_b\lambda) - I_0(B_j r_b\lambda)}{I_1(B_j r_b\lambda)}\right\}$$

Integrating by parts

$$\mathcal{L}^{-1}\left\{\frac{1}{B_j}\,\overline{\eta}(\lambda)\,\frac{I_0(B_j r_b\lambda)}{I_1(B_j r_b\lambda)}\right\} = \frac{1}{B_j}\left\{\eta(z) - \eta(0)T\left(\frac{z}{B_j r_b}\right) - \eta_1(z)T(0) - \frac{1}{B_j r_b}\int_0^z \eta_1(s)T'\left(\frac{z-s}{B_j r_b}\right)ds\right\} \qquad (A6)$$

since $\eta_1(0) = 0$ and where

$$T'\left(\frac{z}{B_j r_b}\right) = \mathcal{L}^{-1}\left\{B_j r_b\lambda\,\frac{I_1(B_j r_b\lambda) - I_0(B_j r_b\lambda)}{I_1(B_j r_b\lambda)}\right\} - T(0)$$

Substituting the asymptotic expansions (A2) for the Bessel functions and letting $\zeta = B_j r_b\lambda$ yield

$$\frac{I_1(\zeta) - I_0(\zeta)}{I_1(\zeta)} = 1 - \frac{e^{\zeta}\left[1 + \sum_{m=1}^{\infty}(-)^m\frac{(0,m)}{(2\zeta)^m}\right] \pm \frac{i}{e^{\zeta}}\left[1 + \sum_{m=1}^{\infty}\frac{(0,m)}{(2\zeta)^m}\right]}{e^{\zeta}\left[1 + \sum_{m=1}^{\infty}(-)^m\frac{(1,m)}{(2\zeta)^m}\right] \mp \frac{i}{e^{\zeta}}\left[1 + \sum_{m=1}^{\infty}\frac{(1,m)}{(2\zeta)^m}\right]}$$

Dividing out the right side of this expression results in

$$1 - \frac{1 + \sum_{m=1}^{\infty}(-)^m\frac{(0,m)}{(2\zeta)^m}}{1 + \sum_{m=1}^{\infty}(-)^m\frac{(1,m)}{(2\zeta)^m}} + e^{-2\zeta}f_1(\zeta) + e^{-4\zeta}f_2(\zeta) + \ldots + e^{-2n\zeta}f_n(\zeta) + \ldots$$

but $\mathcal{L}^{-1}\{e^{-2n\zeta}f_n(\zeta)\}$ is 0 for $z < 2n$ (see e.g. p. 116 of ref. 14), so that these $e^{\ }$ modified terms do not influence $T'(z/B_j r_b)$ for $z/B_j r_b < 2$. Dividing the numerator by the denominator in the expression

$$\frac{1 + \sum_{m=1}^{\infty}(-)^m\frac{(0,m)}{(2\zeta)^m}}{1 + \sum_{m=1}^{\infty}(-)^m\frac{(1,m)}{(2\zeta)^m}}$$

and interpreting the resulting series for T term

by term result in $T\left(\frac{z}{B_j r_b}\right) = -\frac{1}{2}\left(\frac{z}{B_j r_b}\right) - \frac{3}{16}\left(\frac{z}{B_j r_b}\right) - \ldots$ so that $T(0) = 0$. Differentiating $T\left(\frac{z}{B_j r_b}\right)$ results in

$$T'\left(\frac{z}{B_j r_b}\right) = -\frac{1}{2} - \frac{3}{8}\left(\frac{z}{B_j r_b}\right) - \ldots = -W\left(-\frac{z}{B_j r_b}\right) \tag{A7}$$

for $0 \leq \frac{z}{B_j r_b} < 2$. Since

$$\int_0^z \eta_1(s) T'\left(\frac{z-s}{B_j r_b}\right) ds = \int_0^z \eta(s) T'\left(\frac{z-s}{B_j r_b}\right) ds - \eta(0) \int_0^z \frac{\partial T}{\partial s} \frac{\partial s}{\partial\left(\frac{z-s}{B_j r_b}\right)} ds$$

$$= \int_0^z \eta(s) T'\left(\frac{z-s}{B_j r_b}\right) ds - \eta(0) B_j r_b T\left(\frac{z}{B_j r_b}\right)$$

it follows from equations (A6) and (A7) that

$$\mathcal{L}^{-1}\left\{\frac{\overline{\eta}(\lambda)}{B_j} \frac{I_0(B_j r_b \lambda)}{I_1(B_j r_b \lambda)}\right\} = \frac{1}{B_j}\left\{\eta(z) + \frac{1}{B_j r_b}\int_0^z W\left(-\frac{z-s}{B_j r_b}\right)\eta(s)ds\right\} \tag{A8}$$

Combining equations (8), (A3), (A5), and (A8) gives

$$\frac{p_j - p_\infty}{\rho_j U_j^2} = \left(\frac{\rho_\infty U_\infty^2}{\rho_j U_j^2}\frac{1}{B_\infty} + \frac{1}{B_j}\right)\eta(z) - \frac{1}{2r_b}\left(\frac{\rho_\infty U_\infty^2}{\rho_j U_j^2}\frac{1}{B_\infty^2} - \frac{1}{B_j^2}\right)\int_0^z \eta(s)ds$$

$$+ \frac{3}{8r_b}\left(\frac{\rho_\infty U_\infty^2}{\rho_j U_j^2}\frac{B_j}{B_\infty^3} + \frac{1}{B_j^2}\right)\int_0^z \left(\frac{z-s}{B_j r_b}\right)\eta(s)ds$$

$$- \frac{3}{16r_b}\left(\frac{\rho_\infty U_\infty^2}{\rho_j U_j^2}\frac{B_j^2}{B_\infty^4} - \frac{1}{B_j^2}\right)\int_0^z \left(\frac{z-s}{B_j r_b}\right)^2 \eta(s)ds$$

$$+ \frac{21}{256r_b}\left(\frac{\rho_\infty U_\infty^2}{\rho_j U_j^2}\frac{B_j^3}{B_\infty^5} + \frac{1}{B_j^2}\right)\int_0^z \left(\frac{z-s}{B_j r_b}\right)^3 \eta(s)ds + \ldots \tag{9}$$

for $0 < \frac{z}{B_j r_b} < 2$.

REFERENCES

1. Squire, H. B.: Jet Flow and Its Effect on Aircraft. Aircraft Eng., vol. XXII, no. 253, Mar. 1950, pp. 62-67.

2. Falk, H.: The Influence of the Jet of a Propulsion Unit on Nearby Wings. NACA TM 1104, 1946.

3. Englert, Gerald W., and Luidens, Roger W.: Wind-Tunnel Technique for Simultaneous Simulation of External Flow Field About Nacelle Inlet and Exit Airstreams at Supersonic Speeds. NACA TN 3881, 1957.

4. Cortright, Edgar M., Jr.: Some Aerodynamic Considerations of Nozzle-Afterbody Combinations. Aero. Eng. Rev., vol. 15, no. 9, Sept. 1956, pp. 59-65.

5. Platt, J. T.: A Method of Estimating the Pressure on a Wide Base Annulus Separating a Sonic Jet from an External Supersonic Stream. Rep. AE 115, English Elec. Co., Ltd., Jan. 1959.

6. Love, Eugene S., and Grigsby, Carl E.: Some Studies of Axisymmetric Free Jets Exhausting from Sonic and Supersonic Nozzles Into Still Air and Into Supersonic Streams. NACA RM L54L31, 1955.

7. Love, Eugene S., Woodling, Mildred J., and Lee, Louise P.: Boundaries of Supersonic Axisymmetric Free Jets. NACA RM L56G18, 1956.

8. Love, Eugene S.: An Approximation of the Boundary of a Supersonic Axisymmetric Jet Exhausting into a Supersonic Stream. Jour. of the Aero. Soc., vol. 25, no. 2, Feb. 1958, pp. 130-131.

9. Ward, Gilford Norman: Linearized Theory of Steady High-Speed Flow. Ch. 8, Univ. Press (Cambridge), 1955.

10. Pack, D. C.: The Oscillations of a Supersonic Gas Jet Embedded in a Supersonic Stream. Jour. Aero. Sci., vol. 23, no. 8, Aug. 1956, pp. 747-753; 764.

11. Ince, E. L.: Ordinary Differential Equations. Dover Pub., 1944.

12. Love, Eugene S., and Lee, Louise P.: Shape of Initial Portion of Boundary of Supersonic Axisymmetric Free Jets at Large Jet Pressure Ratios. NACA TN 4195, 1958.

13. Watson, G. N.: A Treatise on the Theory of Bessel Functions. Second ed., Univ. Press (Cambridge), 1944, p. 202.

14. McLachlan, Norman William: Complex Variable and Operational Calculus with Technical Applications. Univ. Press (Cambridge), 1942.

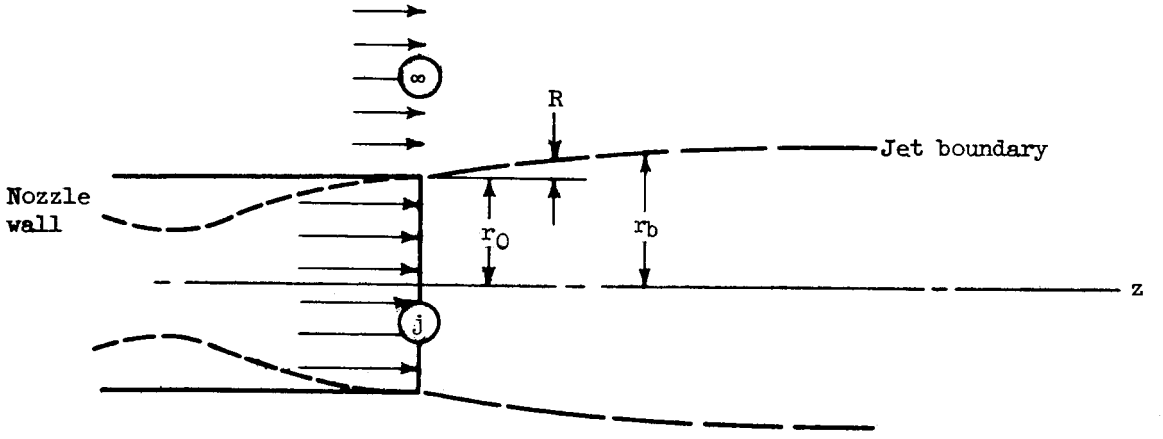

Figure 1. - Linearized flow model.

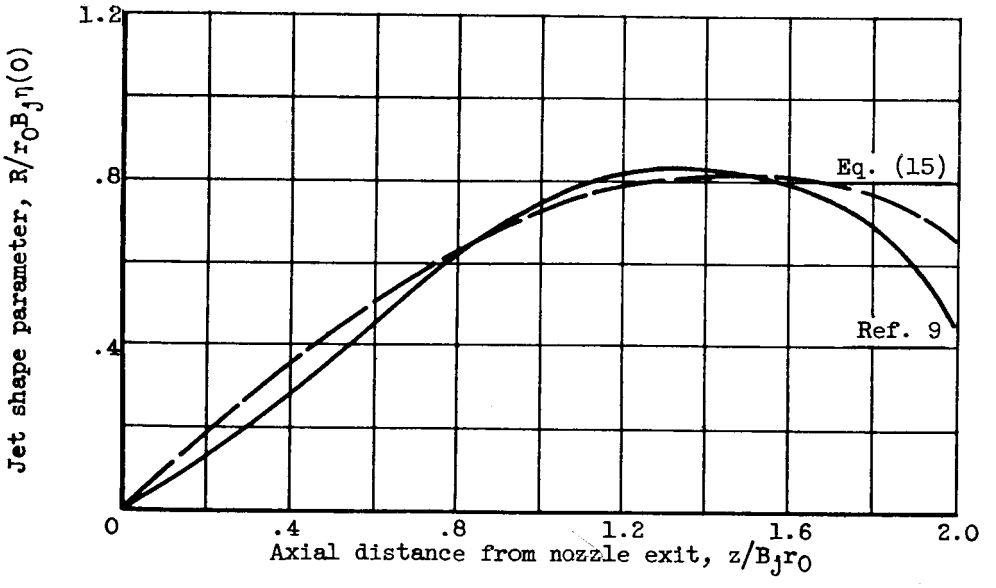

Figure 2. - Comparison of methods of computing jet shape parameter for quiescent surroundings.

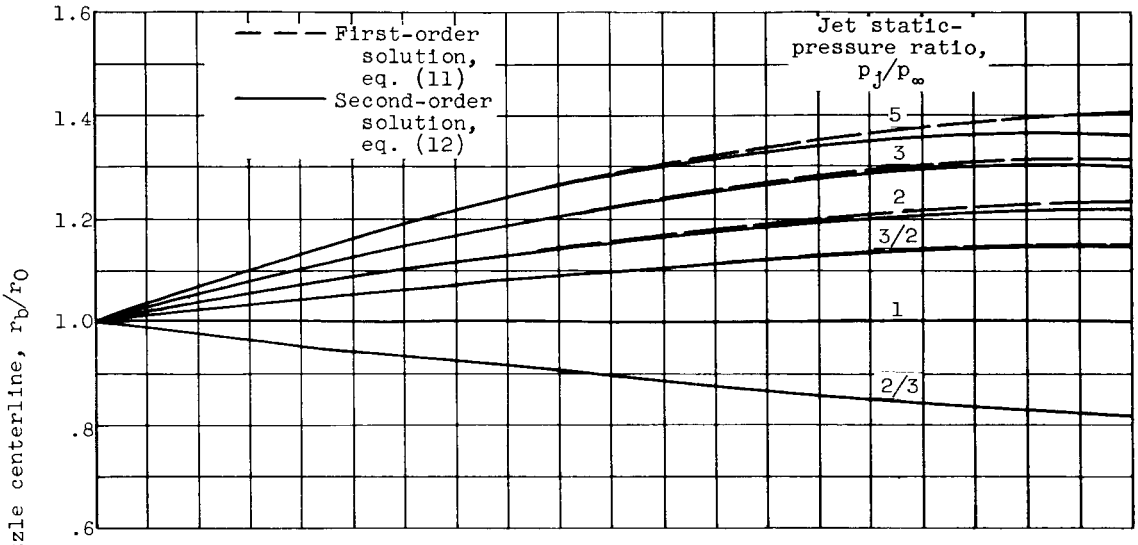

(a) Nozzle-exit and stream Mach numbers, M_j and M_∞, 2.

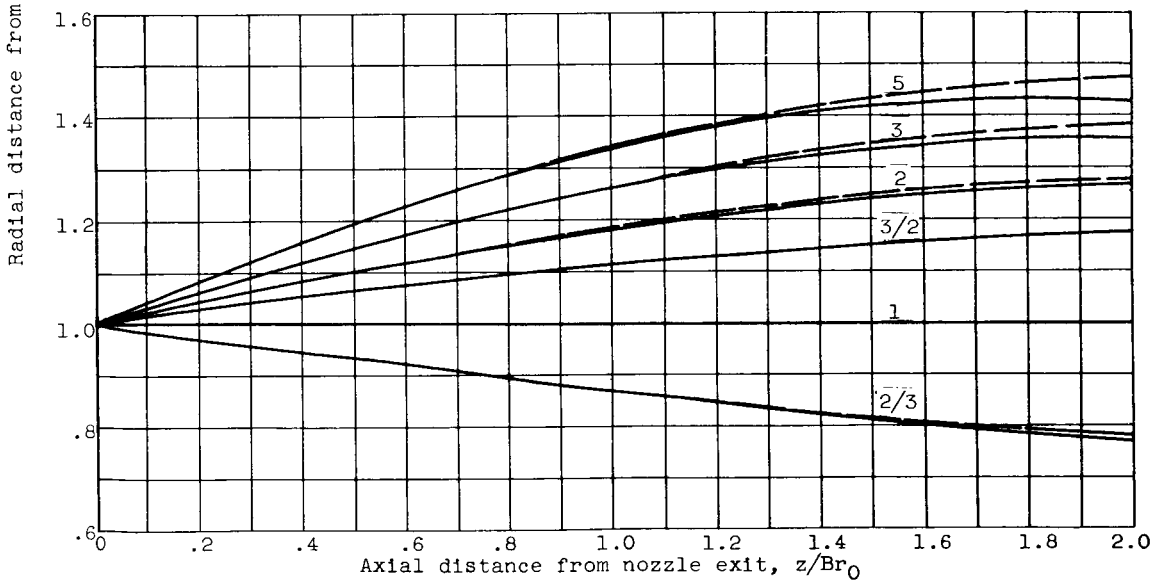

(b) Nozzle-exit and stream Mach numbers, M_j and M_∞, 3.

Figure 3. - Comparison of first- and second-order theory for jet shape. Nozzle-exit and stream specific-heat ratios, γ_j and γ_∞, 1.4; $\eta(0) = \dfrac{1 - p_j/p_\infty}{\gamma M_j^2 a_1}$.

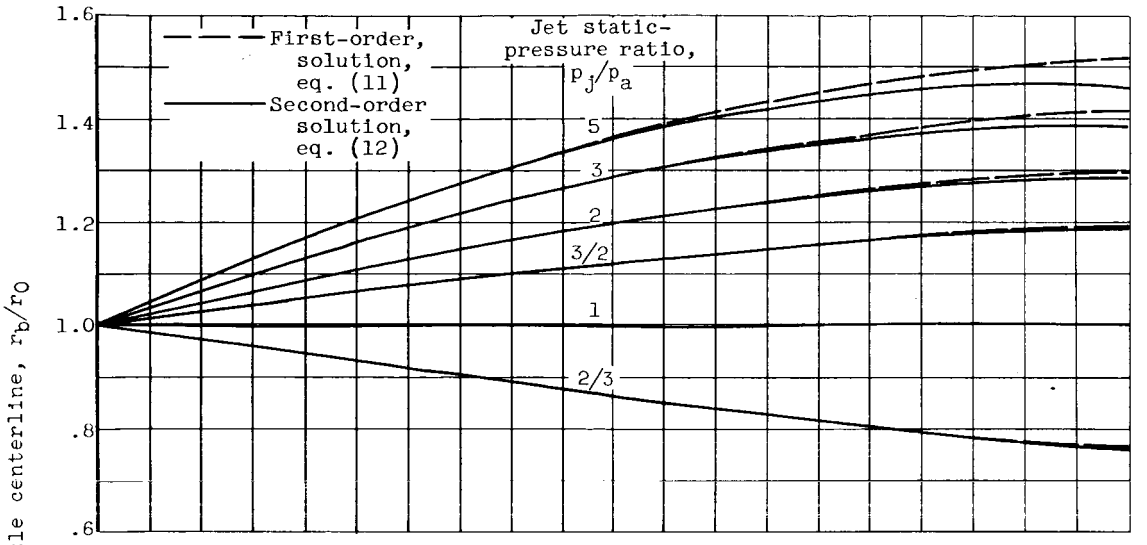

(c) Nozzle-exit and stream Mach numbers, M_j and M_∞, 5.

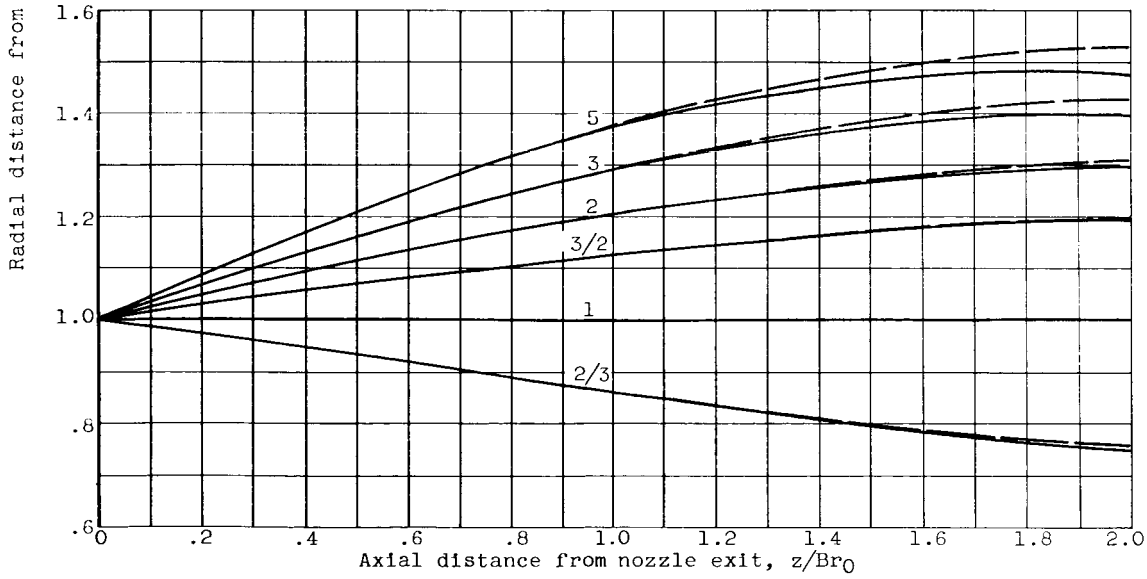

(d) Nozzle-exit and stream Mach numbers, M_j and M_∞, 9.

Figure 3. - Concluded. Comparison of first- and second-order theory for jet shape. Nozzle-exit and stream specific-heat ratios, γ_j and γ_∞, 1.4;

$$\eta(0) = \frac{1 - p_j/p_\infty}{\gamma M_j^2 a_1}.$$

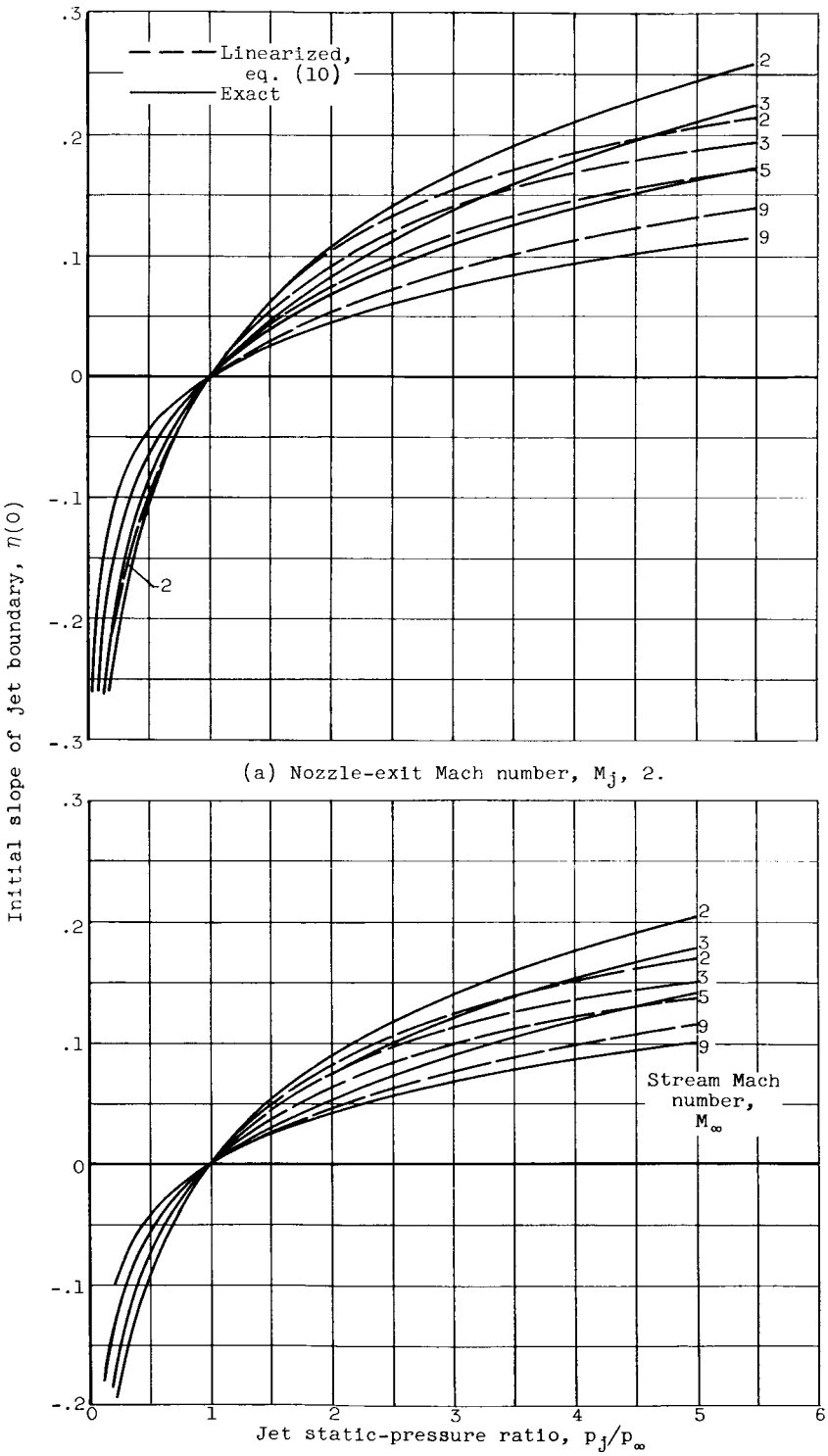

Figure 4. - Comparison of linearized and exact initial slopes of jet boundary. Nozzle-exit and stream specific-heat ratios, γ_j and γ_∞, 1.4; nozzle wall and boattail angles, 0.

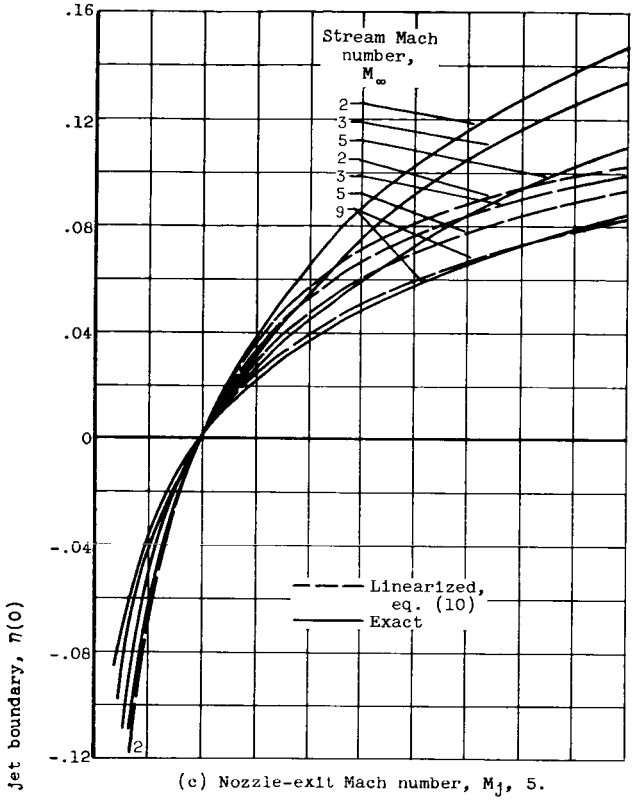

(c) Nozzle-exit Mach number, M_j, 5.

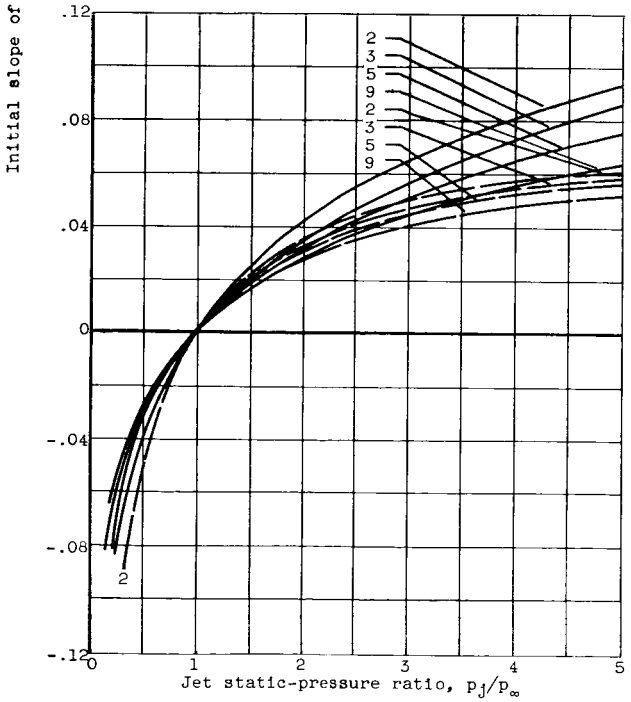

(d) Nozzle-exit Mach number, M_j, 9.

Figure 4. - Concluded. Comparison of linearized and exact initial slopes of jet boundary. Nozzle-exit and stream specific-heat ratios, γ_j and γ_∞, 1.4; nozzle wall and boattail angles, 0.

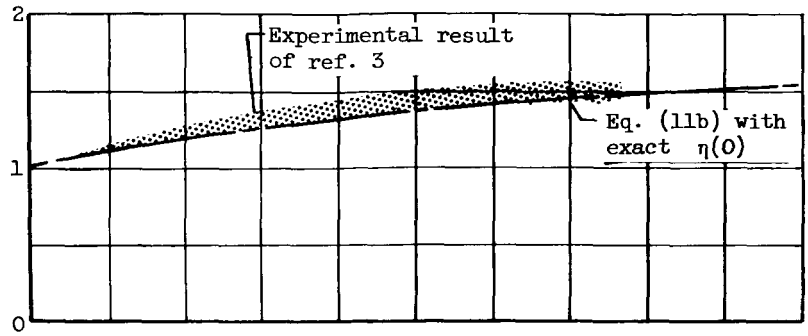

(a) Nozzle-exit Mach number, M_j, 2.29; stream Mach number, M_∞, 3.00; jet static-pressure ratio, p_j/p_∞, 2; nozzle wall angle, 12°; boattail angle, 0.

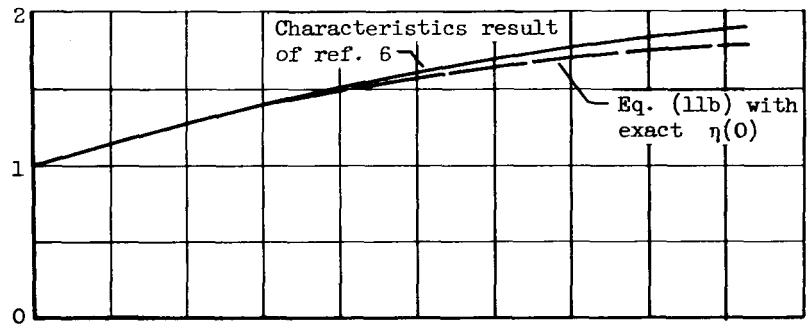

(b) Nozzle-exit Mach number, M_j, 2.38; stream Mach number, M_∞, 3.24; jet static-pressure ratio, p_j/p_∞, 8.96; nozzle wall angle, 12.5°; boattail angle, 9°.

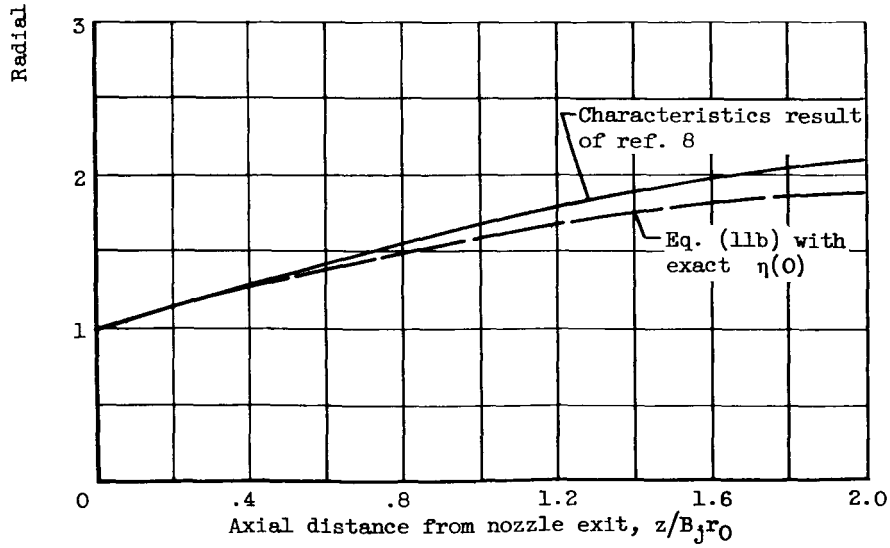

(c) Nozzle-exit Mach number, M_j, 3.0; stream Mach number, M_∞, 6.0; jet static-pressure ratio, p_j/p_∞, 12.23; nozzle wall angle, 12.5°; boattail angle, 0.

Figure 5. - Jet contour for supersonic external flow.

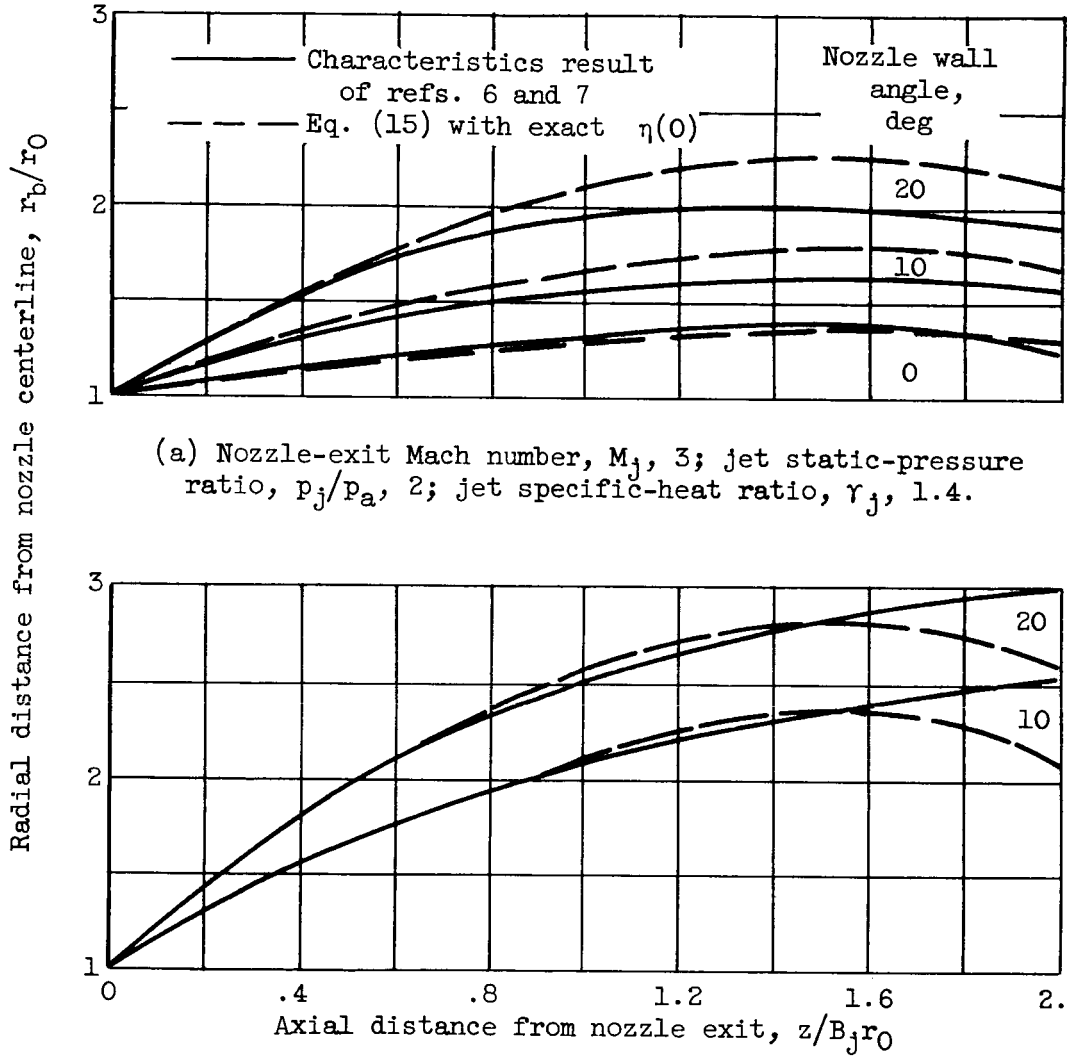

(a) Nozzle-exit Mach number, M_j, 3; jet static-pressure ratio, p_j/p_a, 2; jet specific-heat ratio, γ_j, 1.4.

(b) Nozzle-exit Mach number, M_j, 3; jet static-pressure ratio, p_j/p_a, 5; jet specific-heat ratio, γ_j, 1.4.

Figure 6. - Jet contour for quiescent surroundings.

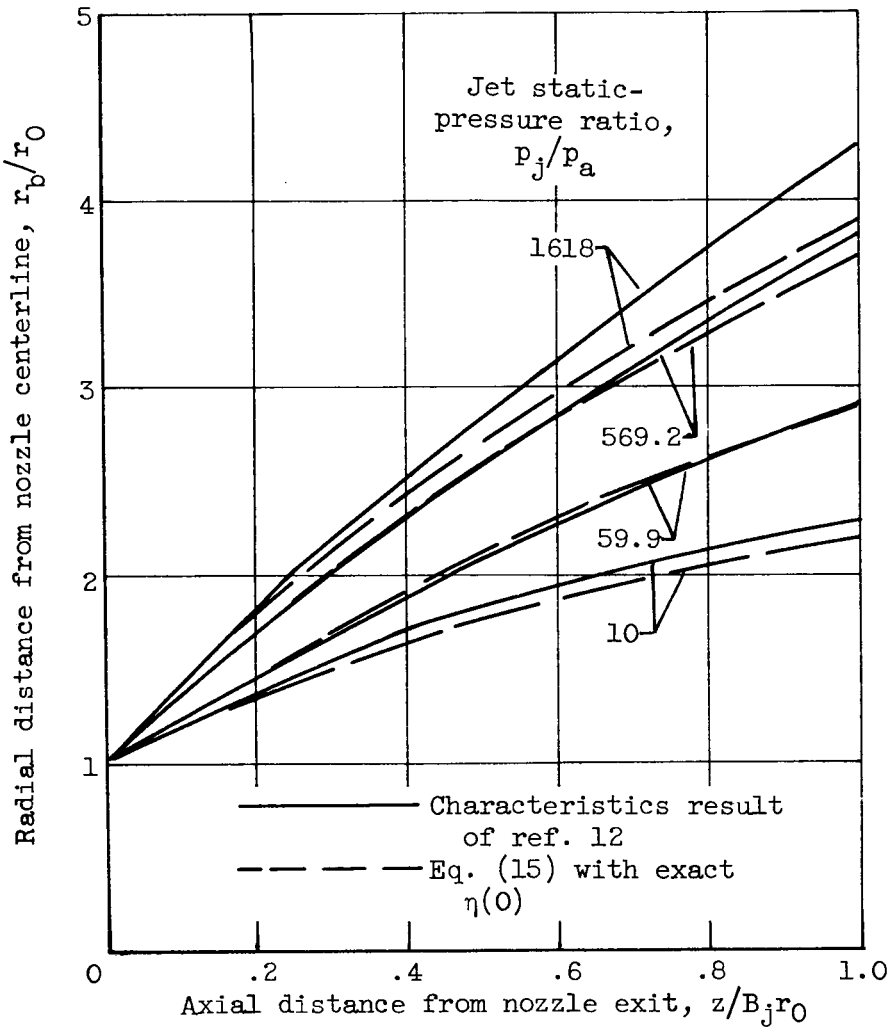

(c) Nozzle-exit Mach number, M_j, 2.5; jet specific-heat ratio, γ_j, 1.667; nozzle wall angle, 15°.

Figure 6. - Concluded. Jet contour for quiescent surroundings.

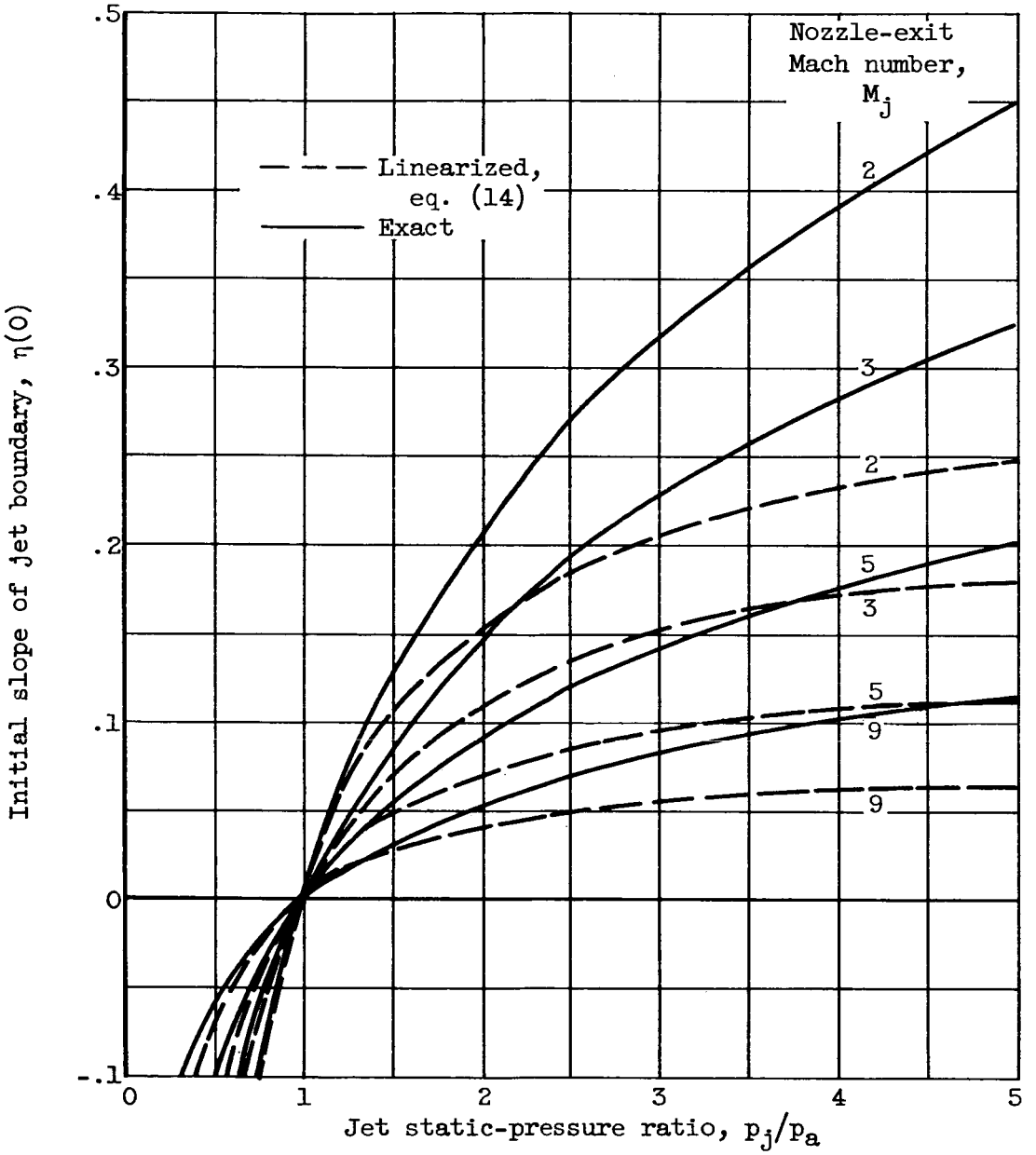

Figure 7. - Comparison of linearized and exact initial slope of jet boundary. Quiescent external field; jet specific-heat ratio, γ_j, 1.4; nozzle wall and boattail angles, 0.

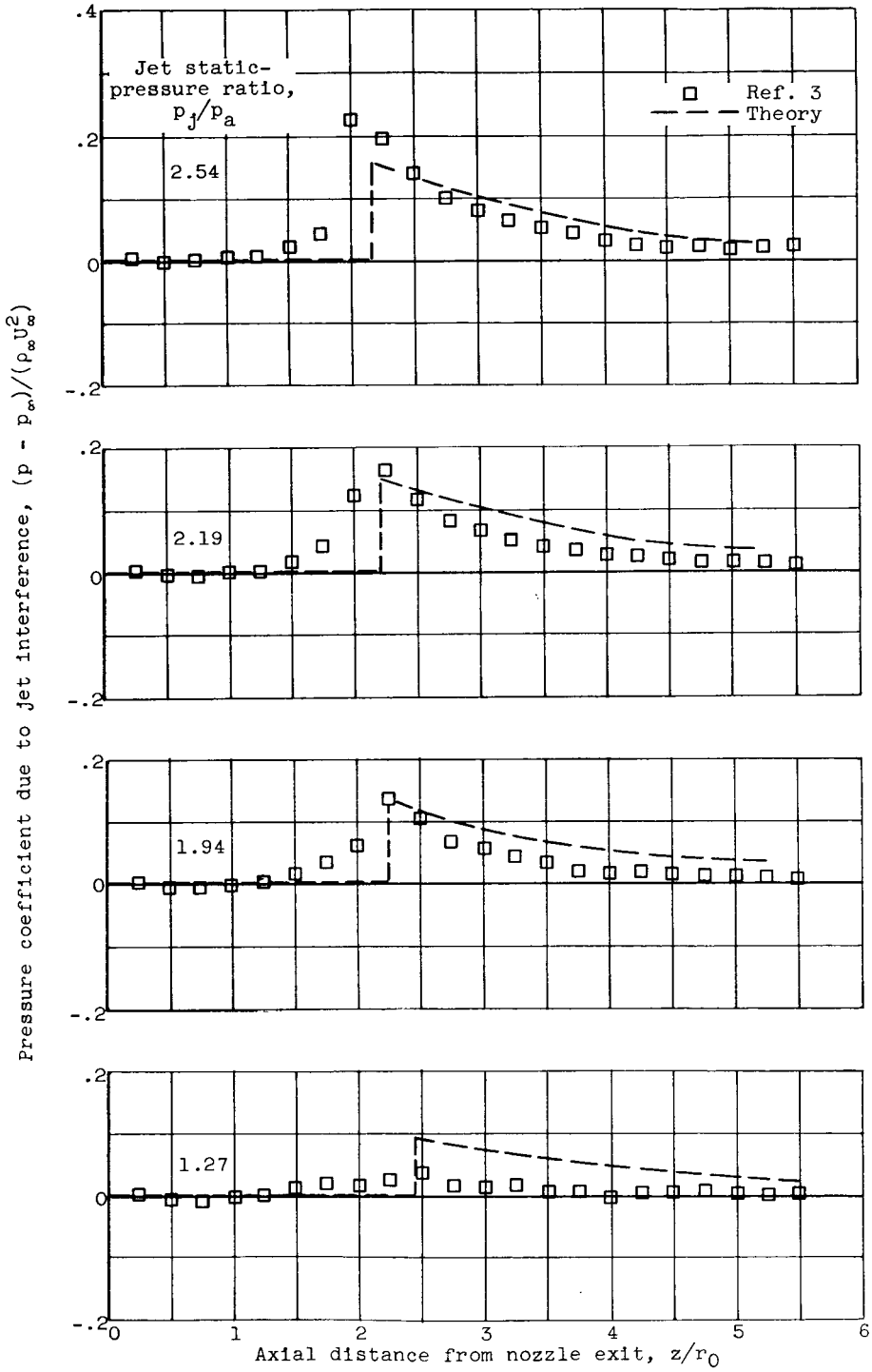

(a) Stream Mach number, M_∞, 3.

Figure 8. - Influence of jet on adjacent surface. Nozzle-exit Mach number, M_j, 2.29; jet and stream specific-heat ratios, γ_j and γ_∞, 1.4; radial distance from nozzle centerline, r/r_0, 2.

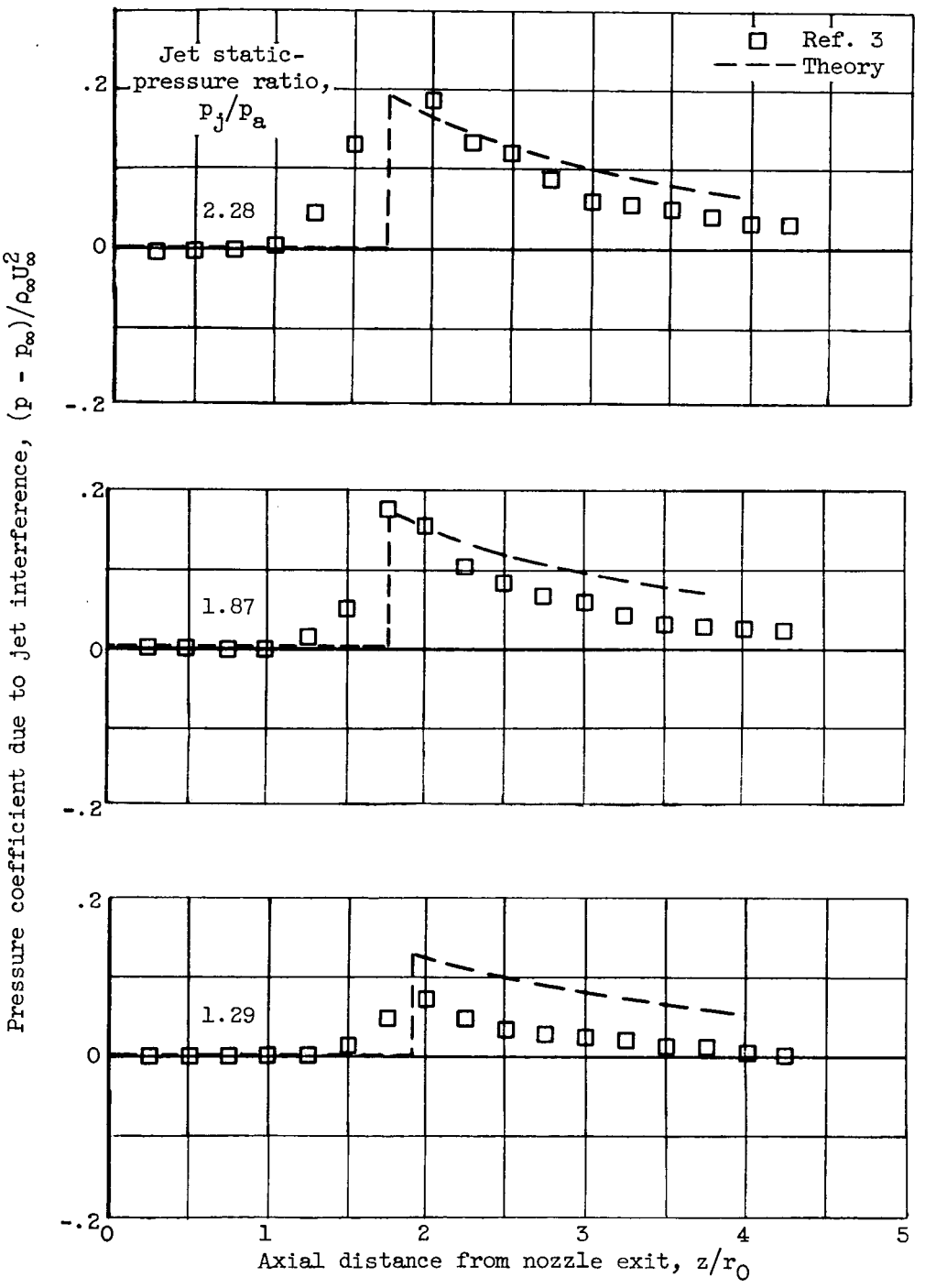

(b) Stream Mach number, M_∞, 2.5.

Figure 8. - Concluded. Influence of jet on adjacent surface. Nozzle-exit Mach number, M_j, 2.29; jet and stream specific-heat ratios, γ_j and γ_∞, 1.4; radial distance from nozzle centerline, r/r_0, 2.